Finite-Volume Solutions to the Water-Hammer Equations in Conservation Form Incorporating Dynamic Friction Using the Godunov Scheme

Aboudou Seck[1]; Musandji Fuamba, Ph.D., M.ASCE[2]; and René Kahawita, Ph.D.[3]

Abstract: Although derived from the principles of conservation of mass and momentum, the water-hammer equations integrating dynamic friction are almost never expressed in conservative form. This is because the pressure and volume discharge are used as variables but these are not conserved quantities, especially when the one-dimensional velocity profile is distorted from its assumed steady state shape due to the large accelerations imposed on the fluid particles across the cross section. This paper presents the derivation of the water-hammer equations in conservation form incorporating dynamic friction. With the dynamic friction taken into account, a source term appears in the basic partial differential equations as presented by Guinot. The numerical algorithm implements the Godunov approach to one-dimensional hyperbolic systems of conservation laws on a finite-volume stencil. Two case studies are used to illustrate the influence of the various formulations. A comparative study between the analytical solution, the numerical solution with quasi-steady friction only, the numerical solution with dynamic friction, and the measurements has been presented. The results indicate that the dynamic friction formulation reduces the peak water hammer pressures when compared with a quasi-steady representation. **DOI: 10.1061/(ASCE)HY.1943-7900.0001333.**

Author keywords: Hydraulic transients; Water hammer; Unsteady friction; Finite volume; Hyperbolic source term; Riemann problem; Godunov scheme; Wave attenuation.

Introduction

In the preliminary design of hydraulic systems, practicing engineers use a general framework to design equipment to prevent and/or mitigate any excessive pressures caused by water hammer. The detailed design further attempts to refine the preliminary concept to elaborate the complete system response using various tools such as numerical modeling. In general, numerical simulation tools assume that the friction factor is considered steady or quasi-steady; this has the tendency to overestimate the water-hammer peak pressures because the primary mechanism that may significantly affect pressure waveforms is the unsteady friction. This results in oversizing of surge control equipment.

The origin of the theory of water hammer goes back to the contributions of Menabrea (1858), who published a short note on the calculation of water pressures (Anderson 1976). However, because of the mathematical rigor and significant theories presented, the papers of Michaud (1878, 1903), Allievi (1903, 1913, 1932), Schnyder (1932), and Jaeger (1933) have been the source of inspiration for all studies on water hammer. Water hammer in hydropower systems and its stability problems were reviewed by Lescovich (1967), Roche (1975), and Chaudhry (1987). Research by Chaudhry et al. (1985), Finnemore and Franzini (2002), and Azhdari Moghaddam (2004) provide implicit equations for analyzing the water-hammer wave. Chaudhry and Silvaaraya (1992) investigated the stability of water level oscillations during transient conditions in a surge tank. Kim (2010) applied a genetic algorithm (GA) coupled with an impulse response technique to derive the impedance functions for pipe systems equipped with a surge tank. Ramadan and Mustafa (2013) investigated the effects of different parameters such as the friction loss coefficient, tank dimensions, and total discharge on transient overpressures. Seck and Fuamba (2015) have developed the analytical equations to design cylindrical and conical surge tanks, and have provided user-friendly diagrams that are based on the equations developed. Their paper bridges the gap between the design concept and the detailed design phase for surge tanks but cannot be used as a general purpose tool for transient analysis because certain key parameters such as the dynamic friction are not incorporated. Guinot (2003) focused on the theoretical and practical implementation of the Godunov approach to simulate water hammer using finite volumes with steady friction that gives rise to a nonhyperbolic source term.

In general, water-hammer models assume that the friction factor is steady or quasi-steady. However, in transient flows with a constant pipe diameter, the one-dimensional velocity profile is distorted from its assumed steady state shape due to the large accelerations (varying across the cross section) that are imposed on the fluid particles. The equivalent friction then exceeds the value assumed at steady state. Brunone et al. (1991) and subsequently Bergant et al. (2001) decomposed the dynamic friction into the sum of a quasi-steady and unsteady parts. Bergant et al. (2008a, b) have experimentally investigated key parameters (unsteady friction, cavitation, fluid–structure interaction, viscoelastic behavior of the

[1]Ph.D. Student, Dept. of Civil, Geological and Mining Engineering, Polytechnique Montréal, 2500 Chemin de Polytechnique, Montreal, QC, Canada H3C 3A7 (corresponding author). E-mail: aboudou.seck@polymtl.ca

[2]Professor, Dept. of Civil, Geological and Mining Engineering, Polytechnique Montréal, 2500 Chemin de Polytechnique, Montreal, QC, Canada H3C 3A7.

[3]Professor, Dept. of Civil, Geological and Mining Engineering, Polytechnique Montréal, 2500 Chemin de Polytechnique, Montreal, QC, Canada H3C 3A7.

Note. This manuscript was submitted on November 11, 2015; approved on February 22, 2017; published online on May 19, 2017. Discussion period open until October 19, 2017; separate discussions must be submitted for individual papers. This paper is part of the ***Journal of Hydraulic Engineering***, © ASCE, ISSN 0733-9429.

pipe wall, leakage, and blockage) that may affect the pressure waveform predicted by the classical theory of water hammer. Bousso and Fuamba (2013) have numerically represented the unsteady friction in transient two-phase flow with a hyperbolic source term. Shamloo et al. (2015) review a quasi-steady model and four unsteady friction models (Zielke 1968; Vardy and Brown 2003; Trikha 1975; Brunone et al. 1991) for transient pipe flow. The Vardy and Brown model is limited to smooth pipes while the Zielke model is developed for transient laminar flow. The Trikha (1975) model presents a simplification of the Zielke (1968) model. The Brunone model appears to be the only one developed for all types of transient flows and all roughness values. Shamloo and Mousavifard (2015) use a two-dimensional finite-difference method incorporating the k-ω turbulence model to study the dynamics of turbulence during different periods of water hammer in a polymeric pipe. However, comparison of their model with experimental tests reveal that the model underestimates the peak water-hammer pressures, which could pose a significant risk for pipe safety.

Although derived from the principles of conservation of mass and momentum, the water-hammer equations integrating dynamic friction are almost never expressed in conservation form. This is because the presence of the dynamic friction terms preclude presentation in the integral (conservation) form and also cause a source term to appear. The finite-volume method that was developed for hyperbolic equations in conservation form (e.g., the Euler equations in fluid dynamics) has to be adapted to tackle systems that are not in proper conservation form. Hyperbolic systems admit weak solutions in the form of discontinuities or shocks. The treatment of these discontinuities requires special treatment of the flux function to avoid spurious oscillations. A large body of literature is available on finite-volume schemes developed to handle the solution in the vicinity of these shocks. Among the most modern numerical schemes are total variation diminishing (TVD) (Zijlema and Wesseling 1998), essentially nonoscillatory (ENO) (Harten et al. 1987), and weighted essentially nonoscillatory (WENO) schemes (Liu et al. 1994; Jiang and Shu 1995). One limitation of the TVD schemes is unsatisfactory performance near extrema (Osher and Chakravarthy 1984; Titarev and Toro 2003; Park et al. 2010). Essentially nonoscillatory and WENO schemes have been developed to overcome this limitation and provide a better scheme that can handle both sharp interfaces and smooth gradients (Shu 1998). According to Gallerano and Cannata (2011) and Gallerano et al. (2012), ENO and WENO shock capturing higher-order schemes for the solution of hyperbolic systems can be considered as a further development of ideas that gave rise to the TVD schemes. The original contribution of this paper is to present the derivation of the water-hammer equations in conservation form incorporating dynamic friction. The hyperbolic system is then solved using a finite-volume scheme. The Godunov scheme was retained to obtain the numerical solutions to the present problem.

It is hoped that this paper will help practical engineers who are at the detailed design phase to further safely optimize any incorporated surge controls by assisting in the development and numerical simulation of the water-hammer equations with dynamic friction.

Methodology

This paper focuses on implementation of the Godunov approach to one-dimensional hyperbolic systems of conservation laws that describe the phenomenon of water-hammer. It is first order accurate in both space and time. In the present context, given the simple geometry, the basic Godunov scheme is considered adequate by the authors. First, the computation of the fluxes is detailed followed by a description of the complete numerical algorithm. Finally, two case studies are investigated with comparisons being made between an analytical solution, the numerical solution with quasi-steady friction, the numerical solution with dynamic friction, and experimental results.

Governing Equations

For a pipe of constant cross section, the one-dimensional flow equations presented in vector form (Guinot 2003) are

$$\frac{\partial \mathbf{U}}{\partial t}+\frac{\partial \mathbf{F}}{\partial x}=\mathbf{S}$$
$$\mathbf{U}=\begin{bmatrix}\mu\\ Q_m\end{bmatrix},\qquad \mathbf{F}=\begin{bmatrix}Q_m\\ A_0 p\end{bmatrix},\qquad \mathbf{S}=\begin{bmatrix}0\\ -f|V|V\end{bmatrix} \tag{1}$$

where t = time; x = unit vector in the x-direction; $\mathbf{U}$ = flow variable vector; $\mathbf{F}$ = flux vector in the x-direction; $\mathbf{S}$ = source term vector; μ = mass of fluid per unit length of pipe; Q_m = mass discharge; A_0 = cross-sectional area of pipe; p = pressure; $\mathbf{V}$ = fluid velocity; and f = friction coefficient dependant on the pipe roughness and the fluid viscosity.

For unsteady friction in transient flow with a constant pipe diameter, the friction factor f is split into the sum of the quasi-steady f_q and unsteady f_u part i.e., $f=f_q+f_u$ as in the model by Brunone et al. (1991) and modified by Bergant et al. (2001)

$$f=f_q+\frac{\sqrt{C^*}D}{2|V|V}\left(\frac{\partial V}{\partial t}+a\,\mathrm{sign}(V)\left|\frac{\partial V}{\partial x}\right|\right) \tag{2}$$

where a = celerity of the pressure waves; D = diameter of the pipe; and C^* = Vardy's shear decay constant depending on the flow regime (Reynolds number R) expressed as

$$C^*=\begin{cases}0.00476 & \text{if laminar flow}\\ \frac{7.41}{\mathsf{R}^{\log(14.3/\mathsf{R}^{0.05})}} & \text{if turbulent flow}\end{cases} \tag{3}$$

Eq. (2) may be rewritten in terms of the flow variables μ and Q_m as

$$f=f_q+\frac{\sqrt{C^*}D}{2|V|V}\left[\left(\frac{1}{\mu}\frac{\partial Q_m}{\partial t}-\frac{Q_m}{\mu^2}\frac{\partial \mu}{\partial t}\right)+a\psi\left(\frac{1}{\mu}\frac{\partial Q_m}{\partial x}-\frac{Q_m}{\mu^2}\frac{\partial \mu}{\partial x}\right)\right] \tag{4}$$

where ψ is expressed as

$$\psi=\begin{cases}+1 & \text{if } V\frac{\partial V}{\partial x}>0\\ -1 & \text{if } V\frac{\partial V}{\partial x}<0\end{cases} \tag{5}$$

For turbulent flow, the Colebrook-White equation may be iteratively solved for the quasi-steady part f_q of the fiction factor

$$\frac{1}{\sqrt{f_q}}=-2\log_{10}\left(\frac{k_S/D}{3.7}+\frac{2.51}{\mathsf{R}\sqrt{f_q}}\right) \tag{6}$$

In which k_S = absolute roughness of the pipe.

Streeter and Wylie (1993) provide the following expression for the celerity (sonic velocity) a in a circular pipe:

$$a=\sqrt{\frac{E_V}{\rho}}\sqrt{\frac{1}{1+\frac{DE_V}{eE}}} \tag{7a}$$

J. Hydraul. Eng., 2017, 143(9): 04017029

where E_V = bulk modulus of elasticity; ρ = mass density; e and E = pipe wall thickness and Young's modulus of elasticity for the pipe material, respectively.

Eq. (7*a*) may be rewritten

$$a = \sqrt{\frac{E_V A_0}{\mu}}\sqrt{\frac{1}{1+\frac{DE_V}{eE}}} \tag{7b}$$

By taking into consideration the unsteady friction, Eq. (1) may be written as

$$\begin{cases} \frac{\partial \mu}{\partial t} + \frac{\partial Q_m}{\partial x} = 0 \\ \frac{\partial Q_m}{\partial t} + \frac{\partial}{\partial x}\left[\frac{2\mu}{2\mu+\sqrt{C^*}D} A_0 p\right] - \frac{\sqrt{C^*}D}{2\mu+\sqrt{C^*}D} a\psi V \frac{\partial \mu}{\partial x} \cdots \\ + \frac{\sqrt{C^*}D}{2\mu+\sqrt{C^*}D}(a\psi - V)\frac{\partial Q_m}{\partial x} = -\frac{2\mu}{2\mu+\sqrt{C^*}D} f_q |V| V \end{cases} \tag{8}$$

In pipe flows, the flow velocity V is negligible compared with a (the celerity of the pressure waves). The authors also note that $2\mu/2\mu + \sqrt{C^*}D \approx 1$ because the term $\sqrt{C^*}D$ is negligible compared with 2μ. Eq. (8) may now be rewritten

$$\begin{cases} \frac{\partial \mu}{\partial t} + \frac{\partial Q_m}{\partial x} = 0 \\ \frac{\partial Q_m}{\partial t} + \frac{\partial}{\partial x}(A_0 p) - \frac{\sqrt{C^*}D}{2\mu+\sqrt{C^*}D} a\psi V \frac{\partial \mu}{\partial x} + \frac{\sqrt{C^*}D}{2\mu+\sqrt{C^*}D}(a\psi)\frac{\partial Q_m}{\partial x} = -f_q |V| V \end{cases} \tag{9}$$

In conservation form the governing Eq. (9) may be written, respectively

$$\begin{aligned} &\frac{\partial \mathbf{U}}{\partial t} + \frac{\partial \mathbf{F}}{\partial x} + \mathbf{R}\frac{\partial \mathbf{U}}{\partial x} = \mathbf{S} \\ &\mathbf{U} = \begin{bmatrix} \mu \\ Q_m \end{bmatrix}, \qquad \mathbf{F} = \begin{bmatrix} Q_m \\ A_0 p \end{bmatrix} \\ &\mathbf{R} = ka\psi \begin{bmatrix} 0 & 0 \\ -V & 1 \end{bmatrix}, \qquad \mathbf{S} = \begin{bmatrix} 0 \\ -f_q |V| V \end{bmatrix} \end{aligned} \tag{10}$$

where $k = \sqrt{C^*}D/2\mu + \sqrt{C^*}D$

$$\begin{aligned} &\frac{\partial \mathbf{U}}{\partial t} + \mathbf{A}\frac{\partial \mathbf{U}}{\partial x} + \mathbf{R}\frac{\partial \mathbf{U}}{\partial x} = \mathbf{S} \\ &\mathbf{A} = \begin{bmatrix} 0 & 1 \\ k\frac{A_0 p}{\mu} + a^2 & 0 \end{bmatrix} = \begin{bmatrix} 0 & 1 \\ a^2 & 0 \end{bmatrix} \end{aligned} \tag{11}$$

This is the general form of the water-hammer equations with unsteady friction.

In Eq. (11), $\mathbf{A} = \partial \mathbf{F}/\partial \mathbf{U}$ is the Jacobian matrix of $\mathbf{F}$ with respect to the matrix $\mathbf{U}$. In the expression for the matrix $\mathbf{A}$, $kA_0 p/\mu \ll a^2$. The general Eq. (10) is equivalent to the Guinot Eq. (1) if unsteady friction is not considered. The inclusion of the unsteady friction results in the appearance of the quasi-linear term $\mathbf{R}\partial \mathbf{U}/\partial x$ in the hyperbolic system [Eq. (10)] thus destroying the integral form of the equations.

The Godunov method is a conservative numerical scheme for solving partial differential equations (PDE) in computational fluid dynamics. This conservative finite-volume method solves an exact or approximate Riemann problem (depending on the friction formulation) at each intercell boundary. It is first order accurate in both space and time. The next section describes the solution process for these equations with the Godunov method.

Numerical Solution

Guinot (2003) as well as Bousso and Fuamba (2013) have provided the procedure for solving PDE's by Godunov's method using the time splitting technique. Eq. (10) is solved in three steps. The first step uses the Guinot solution for the conservation part of the PDE [Eq. (10)]

$$\frac{\partial \mathbf{U}}{\partial t} + \frac{\partial \mathbf{F}}{\partial x} = 0 \tag{12}$$

The second step solves for the nonconservative term of Eq. (10)

$$\frac{\partial \mathbf{U}}{\partial t} + \mathbf{R}\frac{\partial \mathbf{U}}{\partial x} = 0 \tag{13}$$

The final step uses the Toro (2001) and Guinot (2003) treatment of the nonhyperbolic source term of Eq. (10)

$$\frac{\partial \mathbf{U}}{\partial t} = \mathbf{S} \tag{14}$$

Guinot's Solutions at the Internal Cells and at the Boundaries for the Conservation Terms

The conservation component of Eqs. (10) and (12) is the same conservation component as Eq. (1) in Guinot (2003). For the internal cells, Guinot (2003) constructs the Riemann problem $\mathbf{U}(x, t^n)$ and presents the solution $\mathbf{U}_{i+1/2}^{n+1/2}$ of this Riemann problem in Eq. (15) computing the flux $\mathbf{F}_{i+1/2}^{n+1/2}$ between the time intervals t^n and t^{n+1} according to Eq. (16)

$$\mathbf{U}_{i+1/2}^{n+1/2} = \begin{bmatrix} \mu_{i+1/2}^{n+1/2} \\ Q_{m,i+1/2}^{n+1/2} \end{bmatrix} = \frac{1}{2}\begin{bmatrix} \mu_i^n + \mu_{i+1}^n + (Q_{m,i}^n - Q_{m,i+1}^n)/a \\ (\mu_i^n + \mu_{i+1}^n)a + Q_{m,i}^n - Q_{m,i+1}^n \end{bmatrix} \tag{15}$$

$$\mathbf{F}_{i+1/2}^{n+1/2} = \mathbf{F}(\mathbf{U}_{i+1/2}^{n+1/2}) = \begin{bmatrix} Q_{m,i+1/2}^{n+1/2} \\ A_0 p_{\text{ref}} + a^2(\mu_{i+1/2}^{n+1/2} - \mu_{\text{ref}}) \end{bmatrix} \tag{16}$$

where p_{ref} is a reference pressure at which the density ρ_{ref} is known. μ_{ref} is calculated as $\mu_{\text{ref}} = A_0 \rho_{\text{ref}}$.

The flux solutions for a prescribed pressure p_b at the left-hand ($p_{b,L}$) and the right-hand ($p_{b,R}$) boundary are respectively given by

$$\mathbf{F}_{1/2}^{n+1/2} = \begin{bmatrix} Q_{m,1}^n + (\mu_{1/2}^{n+1/2} - \mu_1^n)a \\ A_0 p_{b,L} \end{bmatrix} \tag{17}$$

$$\mathbf{F}_{N+1/2}^{n+1/2} = \begin{bmatrix} Q_{m,N}^n + (\mu_N^n - \mu_{N+1/2}^{n+1/2})a \\ A_0 p_{b,R} \end{bmatrix} \tag{18}$$

In Eqs. (17) and (18), p_b represents a pressure to be prescribed at the boundary. The mass of fluid per unit length of pipe $\mu_{1/2}^{n+1/2}$ (at the left hand) and $\mu_{N+1/2}^{n+1/2}$ (at the right hand) is obtained from the prescribed pressure p_b using

$$\mu_b = \mu_{\text{ref}} + \frac{A_0}{a^2}(p_b - p_{\text{ref}}) \tag{19}$$

The fluxes for a prescribed discharge Q_b at the left-hand and the right-hand boundary are respectively given by

$$\mathbf{F}_{1/2}^{n+1/2} = \begin{bmatrix} Q_b \mu_{1/2}^{n+1/2} / A_0 \\ A_0 p_{\text{ref}} + (\mu_{1/2}^{n+1/2} - \mu_{\text{ref}}) a^2 \end{bmatrix} \tag{20}$$

$$\mathbf{F}_{N+1/2}^{n+1/2} = \begin{bmatrix} Q_b \mu_{N+1/2}^{n+1/2} / A_0 \\ A_0 p_{\text{ref}} + (\mu_{N+1/2}^{n+1/2} - \mu_{\text{ref}}) a^2 \end{bmatrix} \tag{21}$$

where $\mu_{1/2}^{n+1/2}$ in Eq. (20) and $\mu_{N+1/2}^{n+1/2}$ in Eq. (21) are obtained, respectively, from

$$\mu_{1/2}^{n+1/2} = \frac{Q_{m,1}^n - a\mu_1^n}{\frac{Q_b}{A_0} - a} \tag{22}$$

$$\mu_{N+1/2}^{n+1/2} = \frac{Q_{m,N}^n + a\mu_N^n}{\frac{Q_b}{A_0} + a} \tag{23}$$

For all cells, the balance is performed omitting the source term using

$$\mathbf{U}_i^{n+1,x} = \mathbf{U}_i^n + \frac{\Delta t}{\Delta x_i}(\mathbf{F}_{i-1/2}^{n+1/2} - \mathbf{F}_{i+1/2}^{n+1/2}) \tag{24}$$

Solution for the Hyperbolic Source Term at the Internal Cells

The intermediate solution $\mathbf{U}_i^{n+1,x}$ is taken as a starting point for the computation of the hyperbolic source term. This nonhyperbolic source term is solved according to the procedure detailed subsequently.

In Eq. (13), $\mathbf{R} = ka\psi\begin{bmatrix} 0 & 0 \\ -V & 1 \end{bmatrix}$. The two eigenvalues $\lambda^{(1)}$ and $\lambda^{(2)}$ of the matrix $\mathbf{R}$ are therefore

$$\lambda^{(1)} = \begin{cases} 0, & \text{if } \psi = 1 \\ -ka, & \text{if } \psi = -1 \end{cases} \tag{25}$$

$$\lambda^{(2)} = \begin{cases} ka, & \text{if } \psi = 1 \\ 0, & \text{if } \psi = -1 \end{cases} \tag{26}$$

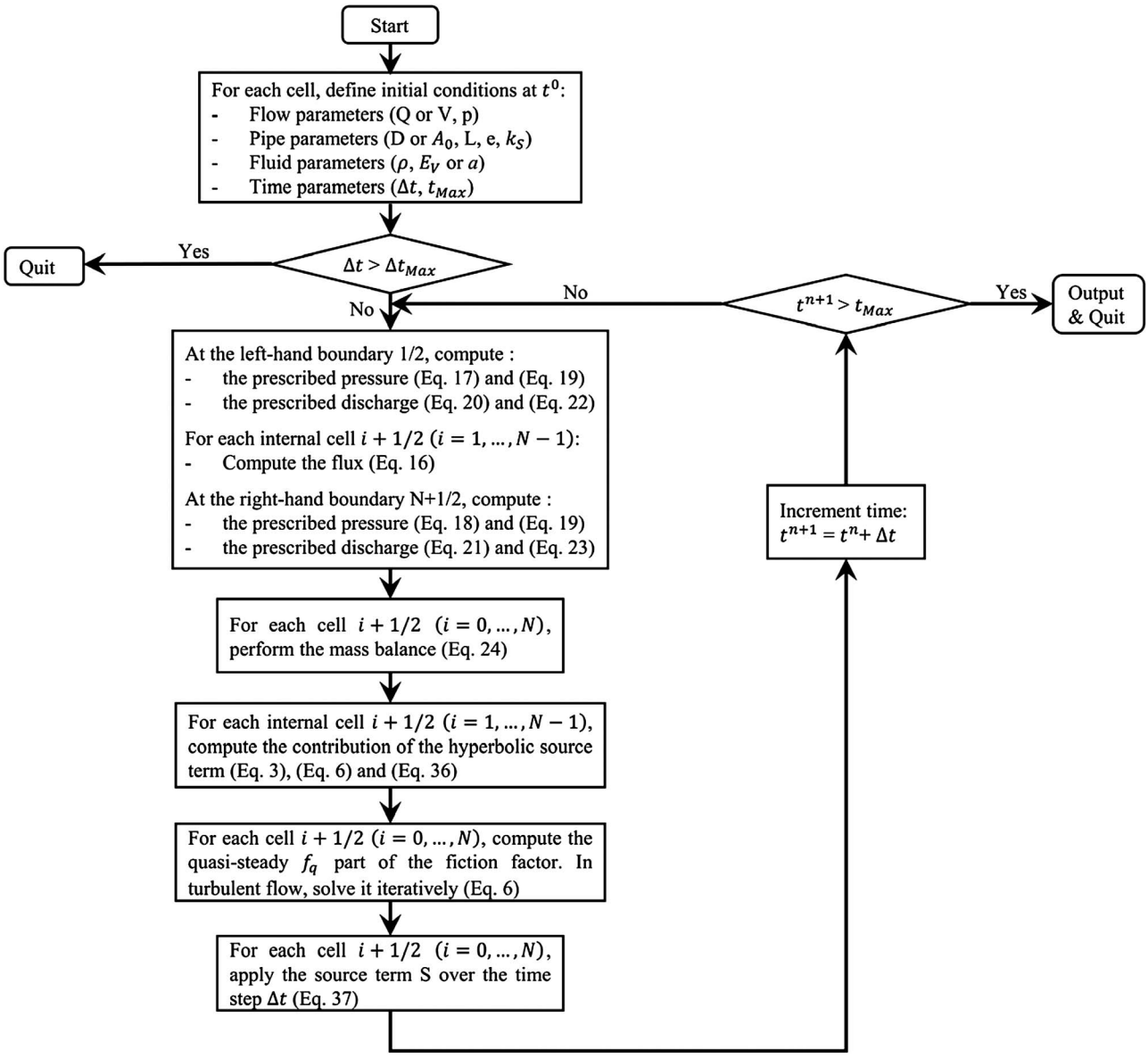

Fig. 1. Schematic of the proposed algorithm

J. Hydraul. Eng., 2017, 143(9): 04017029

The matrix $\mathbf{K}$ of the $\mathbf{R}$ eigenvectors is given by

$$\mathbf{K} = \begin{cases} \begin{bmatrix} 1 & 0 \\ V & 1 \end{bmatrix}, & \text{if } \psi = 1 \\ \begin{bmatrix} 0 & 1 \\ 1 & V \end{bmatrix}, & \text{if } \psi = -1 \end{cases} \tag{27}$$

This yields the following generalized Riemann invariants

$$\left.\begin{array}{l} \frac{d\mu}{1} = \frac{dQ_m}{V}, \text{across } \frac{dx}{dt} = 0 \\ \frac{d\mu}{0} = \frac{dQ_m}{1}, \text{across } \frac{dx}{dt} = ka \end{array}\right\} \quad \text{for } \psi = 1 \tag{28}$$

$$\left.\begin{array}{l} \frac{d\mu}{0} = \frac{dQ_m}{1}, \text{across } \frac{dx}{dt} = -ka \\ \frac{d\mu}{1} = \frac{dQ_m}{V}, \text{across } \frac{dx}{dt} = 0 \end{array}\right\} \quad \text{for } \psi = -1 \tag{29}$$

Noting that $dQ_m = \mu dV + V d\mu$, the system Eqs. (28) and (29) may be rewritten as

$$\left.\begin{array}{l} d\left(\frac{Q_m}{\rho}\right) = 0, \text{across } \frac{dx}{dt} = 0 \\ d\mu = 0, \text{across } \frac{dx}{dt} = ka \end{array}\right\} \quad \text{for } \psi = 1 \tag{30}$$

$$\left.\begin{array}{l} d\mu = 0, \text{across } \frac{dx}{dt} = -ka \\ d\left(\frac{Q_m}{\rho}\right) = 0, \text{across } \frac{dx}{dt} = 0 \end{array}\right\} \quad \text{for } \psi = -1 \tag{31}$$

Consider the Riemann problem as follows:

$$\mathbf{U}(x, t^n) = \begin{cases} \mathbf{U}_i^{n+1,x}, & \text{if } x \le x_{i+1/2} \\ \mathbf{U}_{i+1}^{n+1,x}, & \text{if } x > x_{i+1/2} \end{cases} \tag{32}$$

The solution $\mathbf{U}^h$ of this Riemann problem is given by

for $\psi = 1$

$$\mathbf{U}^h(x, t^{n+1}) = \begin{cases} \mathbf{U}_i^{n+1,x}, & \text{if } x < x_{i+1/2} \\ \mathbf{U}_{i+1/2}^*, & \text{if } x_{i+1/2} \le x < x_{i+1/2} + ka\Delta t \\ \mathbf{U}_{i+1}^{n+1,x}, & \text{if } x \ge x_{i+1/2} + ka\Delta t \end{cases} \tag{33}$$

where

$$\mathbf{U}_{i+1/2}^* = \frac{1}{A_0} \begin{bmatrix} \mu_{i+1}^{n+1,x} \\ A_0^2 \frac{\mu_{i+1}^{n+1,x}}{\mu_i^{n+1,x} \mu_i^{n+1,x}} Q_{m_i}^{n+1,x} \end{bmatrix}$$

for $\psi = -1$

$$\mathbf{U}^h(x, t^{n+1}) = \begin{cases} \mathbf{U}_i^{n+1,x}, & \text{if } x \le x_{i+1/2} - ka\Delta t \\ \mathbf{U}_{i+1/2}^*, & \text{if } x_{i+1/2} - ka\Delta t < x \le x_{i+1/2} \\ \mathbf{U}_{i+1}^{n+1,x}, & \text{if } x > x_{i+1/2} \end{cases} \tag{34}$$

where $\mathbf{U}_{i+1/2}^* = \frac{1}{A_0} \begin{bmatrix} \mu_i^{n+1,x} \\ A_0^2 \frac{\mu_i^{n+1,x}}{\mu_{i+1}^{n+1,x} \mu_{i+1}^{n+1,x}} Q_{m_{i+1}}^{n+1,x} \end{bmatrix}$

The value of $\mathbf{U}_i^{n+1,x}$ is obtained from

$$\mathbf{U}_i^{n+1,x} = \frac{1}{\Delta x_i} \int_{x_{i-1/2}}^{x_{i+1/2}} \mathbf{U}^h(x, t^{n+1}) dx \tag{35}$$

By substituting Eqs. (33) and (34) into Eq. (35), the following equation is obtained:

$$\mathbf{U}_i^{n+1,h} = \left(1 + \frac{ka\psi\Delta t}{\Delta x_i}\right) \mathbf{U}_i^{n+1,x} - \frac{ka\psi\Delta t}{\Delta x_i} \mathbf{U}_{i+1/2}^* \tag{36}$$

Discretization of the Nonhyperbolic Source Term

Taking the provisional solution $\mathbf{U}_i^{n+1,h}$ as the initial state, the solution $\mathbf{U}_i^{n+1}$ of the nonhyperbolic source term is presented by Toro (2001), Guinot (2003), and Bousso and Fuamba (2013) in the following form:

$$\mathbf{U}_i^{n+1} = \mathbf{U}_i^{n+1,h} + \mathbf{S}(\mathbf{U}_i^{n+1,h}) \Delta t \tag{37}$$

where $\mathbf{S}(\mathbf{U}_i^{n+1,h})$ is calculated by using $\mathbf{U}_i^{n+1,h}$ in Eq. (1) of the source term.

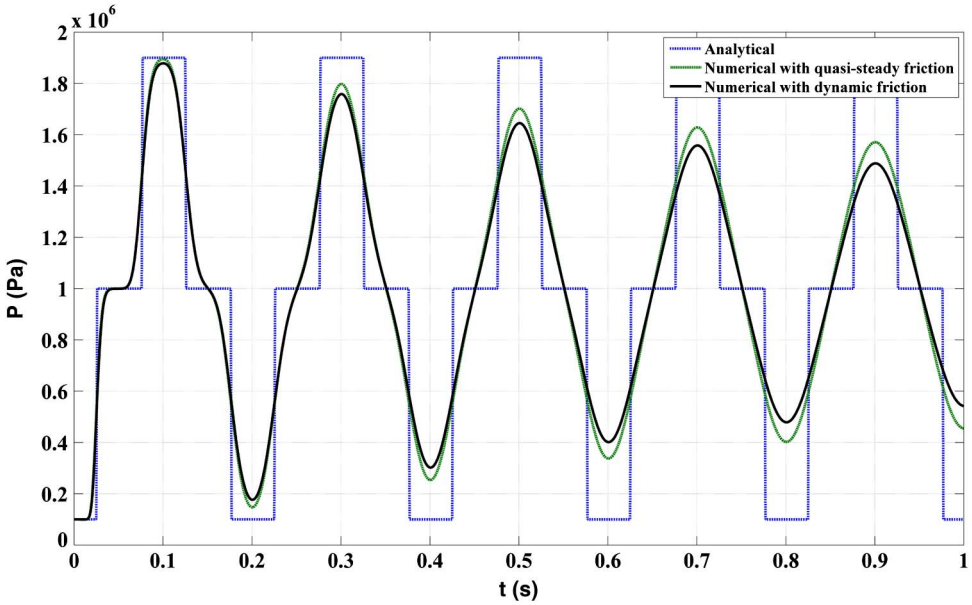

Fig. 2. Comparison of pressure profiles at pipe midpoint ($\Delta t = 0.0002$ s, $N = 50$) between the various formulations for the friction term

J. Hydraul. Eng., 2017, 143(9): 04017029

Computational Time Step

Because the scheme is explicit, the CFL condition for stability must be respected, i.e., the maximum permissible time step Δt_{Max} as presented by Guinot (2003) is as follows:

$$\Delta t_{\text{Max}} = \text{Min}\left[\min_{i=1,\ldots,N}\left(\frac{\Delta x_i}{a}\right), \Delta t_{\text{Max},S}\right] \tag{38}$$

Water-Hammer Wave Attenuation Ratio

The water-hammer wave attenuation ratio η is computed from

$$\eta_i^{n+1}(\%) = \left(1 - \frac{|p_i^{n+1} - p_{b,L}|}{p_{b,L}}\right)100 \tag{39}$$

As t increases ($t \to \infty$) and assuming no pipe failure, the water-hammer wave is completely attenuated in the pipe.

Then, η_i^{n+1} approaches 100% according to

if $t \to \infty$;

$$\eta_1^{\infty} \approx \eta_2^{\infty} \approx \cdots \approx \eta_N^{\infty} \approx \lim_{n\to\infty}\left(1 - \frac{|p_i^{n+1} - p_{b,L}|}{p_{b,L}}\right)100 \approx 100\% \tag{40}$$

Resolution Algorithm

The proposed algorithm is presented in the following (Fig. 1).

Results and Discussion

Two case studies have been simulated: (1) the sudden opening of an upstream valve; and (2) sudden closure of a downstream valve. For the second case study, the numerical results have been compared with data from two recent experimental tests conducted by Brunone

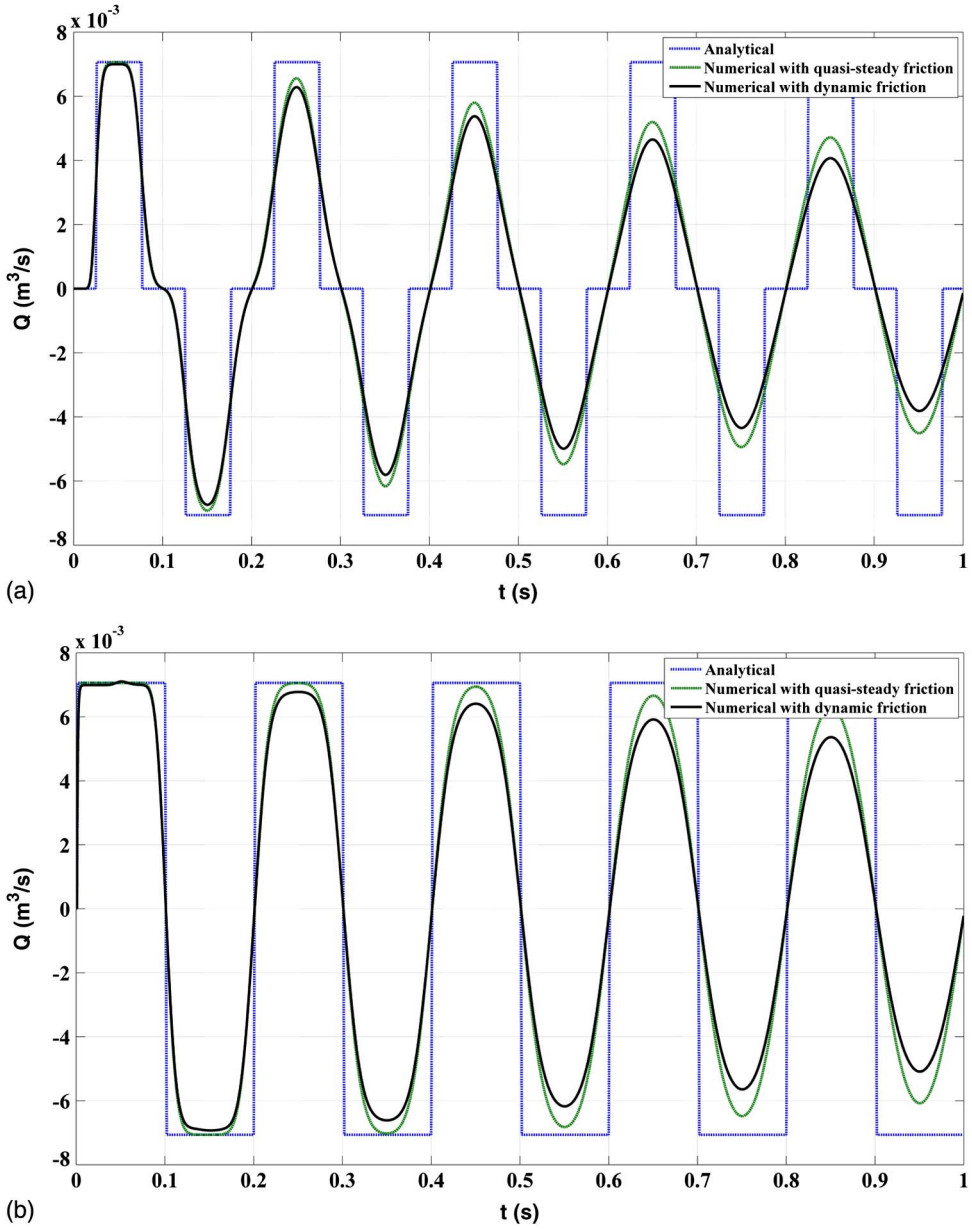

Fig. 3. Comparison of discharge profiles ($\Delta t = 0.0002$ s, $N = 50$) between the various formulations for the friction term: (a) pipe midpoint; (b) downstream of the reservoir

J. Hydraul. Eng., 2017, 143(9): 04017029

and Berni (2010), which are considered to be of good quality. The second case represents the classic case of water hammer.

Case 1: Sudden Opening of an Upstream Valve

Physical Data

The physical data for the case study is adapted from Guinot (2003). The pressure waves and the discharges due to the sudden opening of an upstream valve of a pipe coupled to a reservoir at constant head, higher than that of the prevailing pressure in the pipe is computed. The end of the pipe is considered closed. Initial conditions specify all velocities to be zero. In the Guinot example, the friction is assumed constant, consequently the source term does not appear. The physical data are given as follows (these constitute the initial conditions):

- Pipe diameter: 100 mm;
- Pipe length: 50 m;
- Absolute roughness of the pipe: 0 mm (smooth pipe);
- Sonic velocity (celerity): 1,000 m/s;
- Initial pressure in the pipe: 10^5 Pa;
- Pressure at the left-hand boundary: 10^6 Pa;
- Discharge at the right-hand boundary: 0 m^3/s;
- Initial discharge in the pipe: 0 m^3/s; and
- Water density: 1,000 kg/m^3.

Results and Discussion

The equations for water hammer with unsteady friction were solved using the Godunov scheme detailed previously. In keeping with the objectives of this paper, results were obtained for the analytical resolution, the numerical solution with quasi-steady friction only and the numerical solution with dynamic friction. A time step of $\Delta t = 0.0002$ s was used. Comparison between the results indicates that the inclusion of all components of the friction has an influence on the pressure profiles at pipe midpoint (Fig. 2) and the flow oscillation profiles at pipe midpoint and at the downstream end [Figs. 3(a and b)].

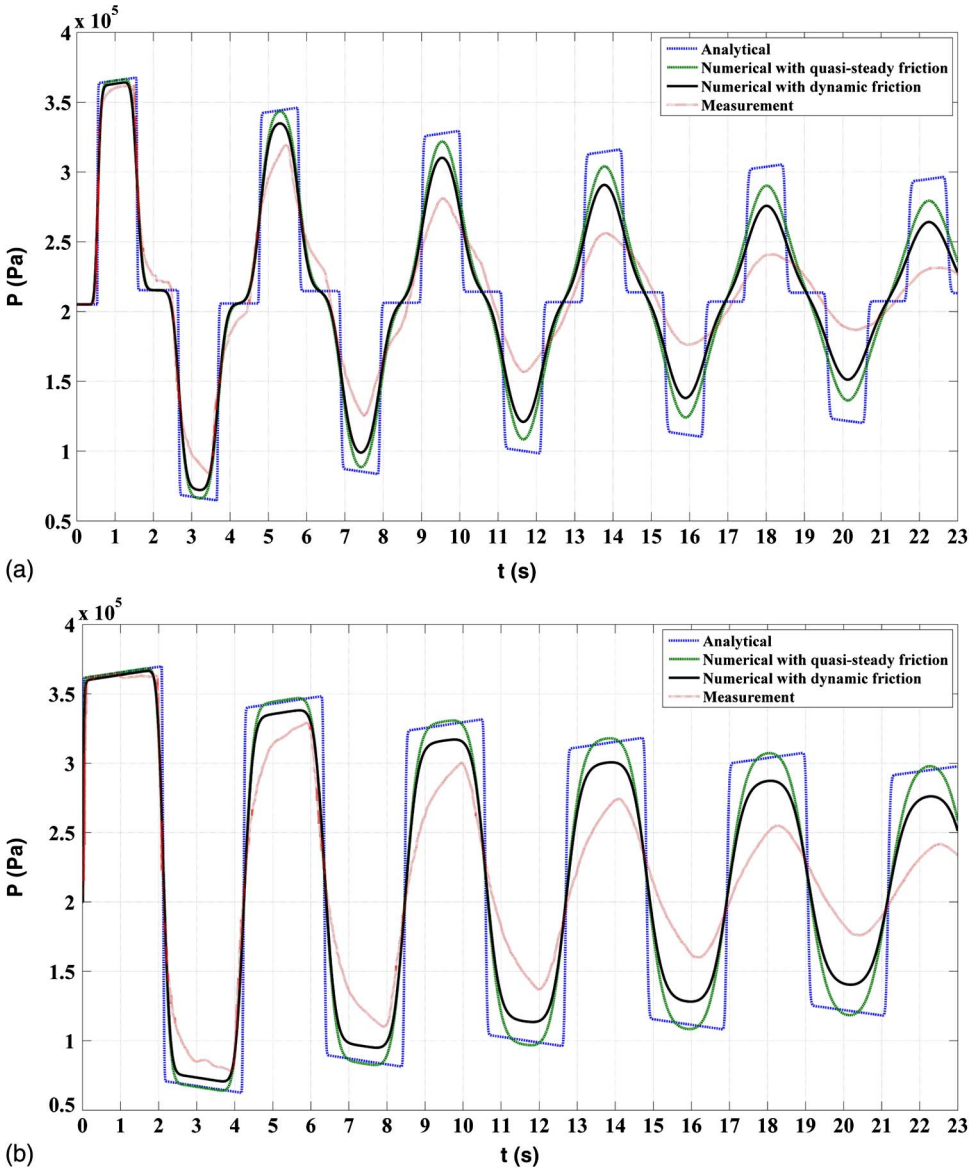

Fig. 4. Test no. 1: comparison of pressure profiles ($\Delta t = 0.002$ s, $N = 100$) between the various formulations for the friction term: (a) Section no. 2; (b) Section no. 3

Because of damping, the waves will be of decreasing amplitude until the final equilibrium pressure is reached. Also, the dynamic friction tends to rapidly attenuate the magnitude of the overpressures. Comparisons at the middle of the pipe and at the downstream end indicate that inclusion of the dynamic friction causes the peak pressure to decay at a rate faster than that with the quasi-steady friction term only.

Case 2: Sudden Closure of a Downstream Valve

Experimental Setup

The results of experimental studies conducted by Brunone and Berni (2010) are compared with the computational results. For two cases of initial conditions, a transient event is initiated by the rapid closure of a downstream valve in a pipe coupled to a constant head reservoir under initially steady flow conditions. The experimental setup is composed of a 352 m long pipe with an inner diameter of 0.0933 m and a thickness of 8.9 mm that connects an upstream the air vessel that is at a (constant) head. The celerity has been estimated as equal to 332.53 m/s. The pressure waves and discharge have been computed and compared with the corresponding experimental values at Section no. 1 (distance $x = 13.76$ m downstream the reservoir), Section no. 2 (distance $x = 180$ m downstream of reservoir), and Section no. 3 (just upstream of the valve).

The initial conditions for Test no. 1 and Test no. 2 are given as follows:

1. Test no. 1
   - Reynolds number: 45200;
   - Initial discharge in the pipe: 3.32 L/s;
   - Pressure at the reservoir: 21.45 m; and
   - Pressure at section no. 3: 20.35 m.
2. Test no. 2
   - Reynolds number: 60700;
   - Initial discharge in the pipe: 4.46 L/s;
   - Pressure at the reservoir: 20.95 m; and
   - Pressure at section no. 3: 19.12 m.

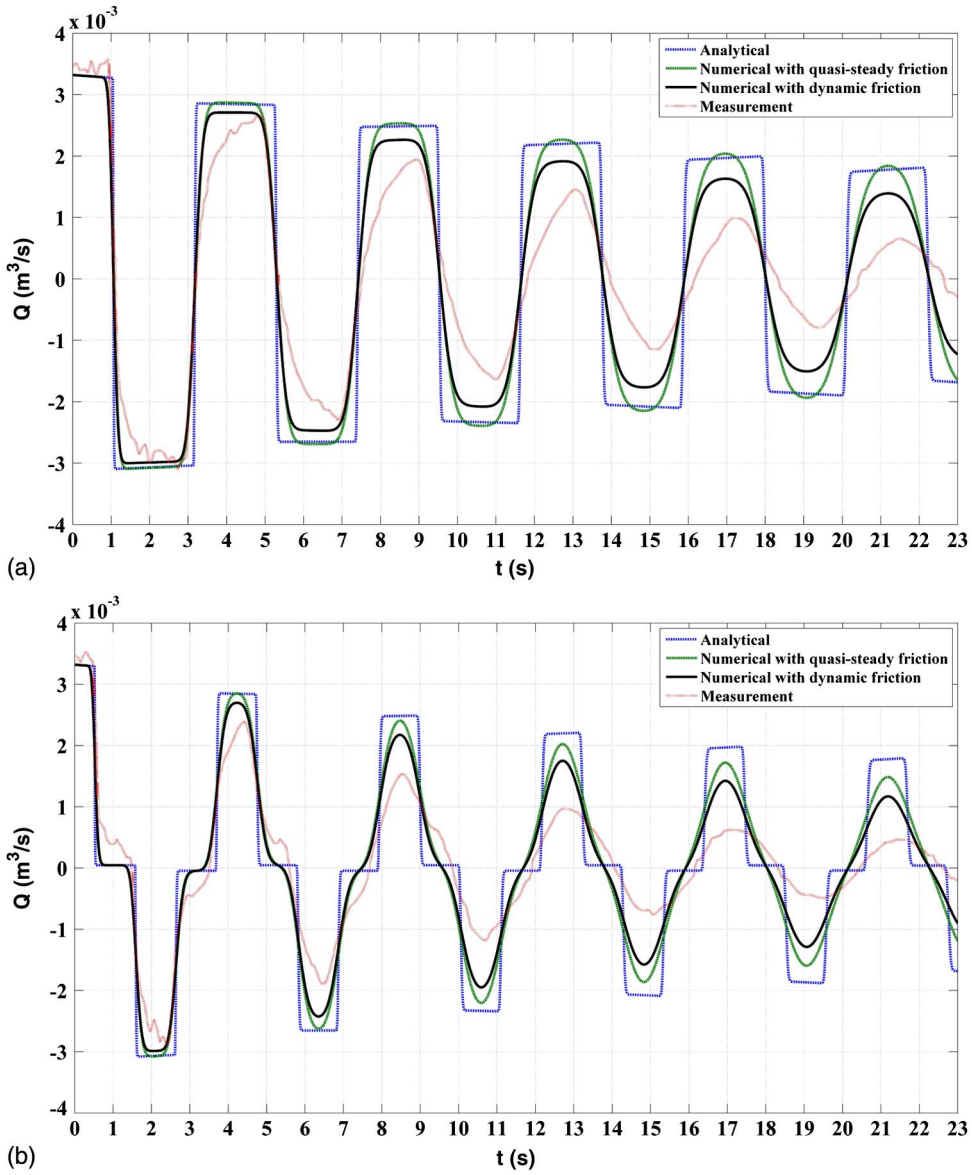

Fig. 5. Test no. 1: comparison of discharge profiles ($\Delta t = 0.002$ s, $N = 100$) between the various formulations for the friction term: (a) Section no. 1; (b) Section no. 2

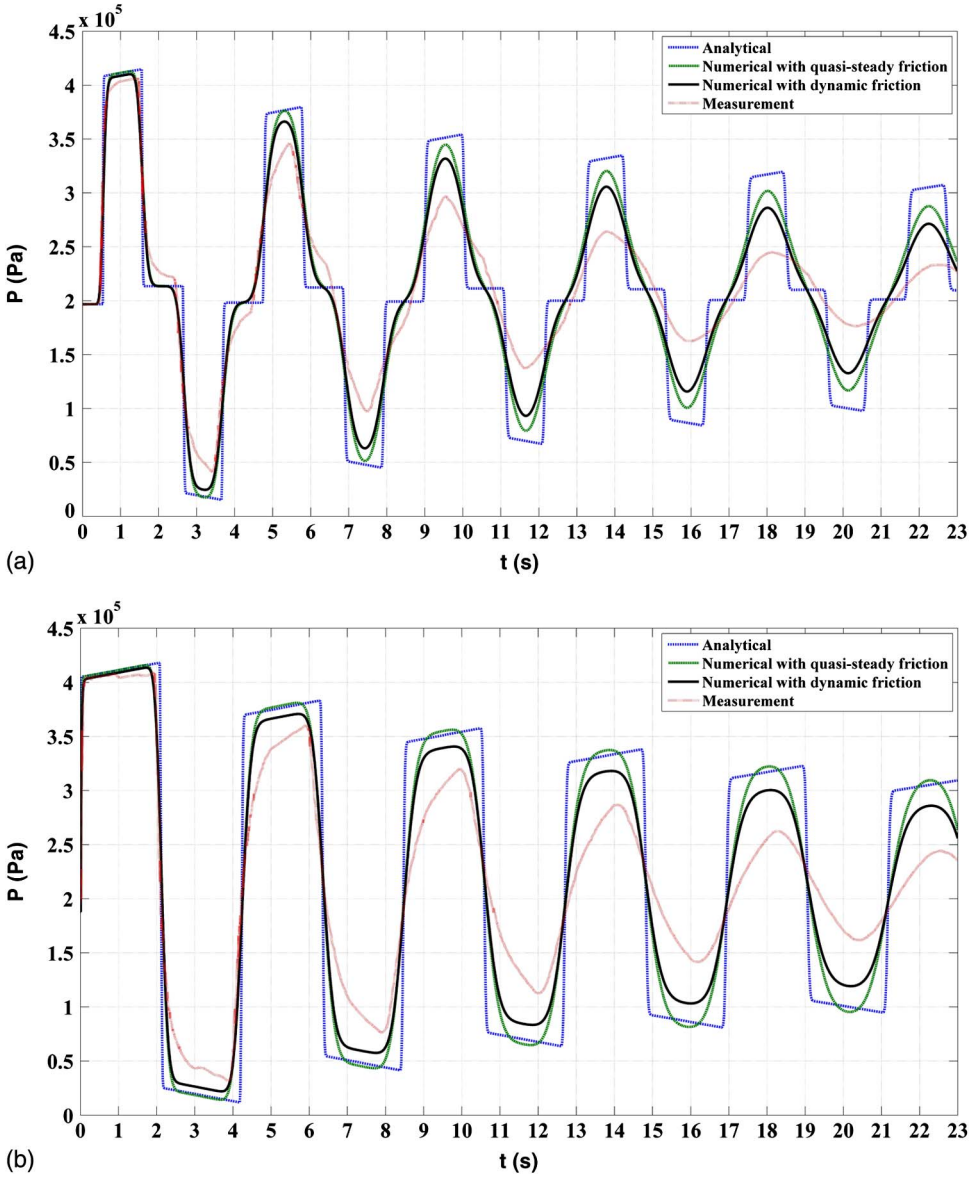

Fig. 6. Test no. 2: comparison of pressure profiles ($\Delta t = 0.002$ s, $N = 100$) between the various formulations for the friction term: (a) Section no. 2; (b) Section no. 3

Results and Discussion

The water-hammer equations with unsteady friction were solved using the Godunov scheme detailed previously. In keeping with the objectives of this paper, results were obtained for the analytical resolution, the numerical solution with quasi-steady friction only, and the numerical solution with dynamic friction using a time step of $\Delta t = 0.002$ s. These results are compared with the experimental measurements. Comparison of the results (Figs. 4–7) indicates that the inclusion of all components of the friction has an influence on the pressure profiles [Figs. 4(a and b) and 6(a and b)] and the flow oscillation profiles [Figs. 5(a and b) and 7(a and b)]. At the valve [Figs. 4(b) and 6(b)] the peak pressures are shown as sloping upward in high pressure and downward in low pressure. The quasi-steady friction model and dynamic friction model are able to reproduce almost exactly the evolution of the typical shape of the pressure oscillations. However, the quasi-steady friction model underestimates the damping and dispersion predicted by the physically more accurate dynamic friction model. The dynamic friction tends to rapidly attenuate the magnitude of the overpressures. At the middle of the pipe and at the downstream end, inclusion of the dynamic friction causes the peak pressure to decay at a faster rate than that with the quasi-steady friction term only. It is expected that better agreement between measured and computed dynamic friction profiles would be obtained if other key parameters are properly modeled and incorporated into the formulation. The resolution will be able to better capture discontinuities in the computed profiles.

Conclusions and Recommendations

The water-hammer equations in conservation form incorporating dynamic friction is developed and numerically solved using a finite-volume formulation. The computational algorithm based on the Godunov scheme for one-dimensional hyperbolic systems is presented in some detail. Introduction of the dynamic friction results in the appearance of a source term in the hyperbolic system of governing partial differential equations. Two case studies have been presented to compare and contrast the separate impacts of

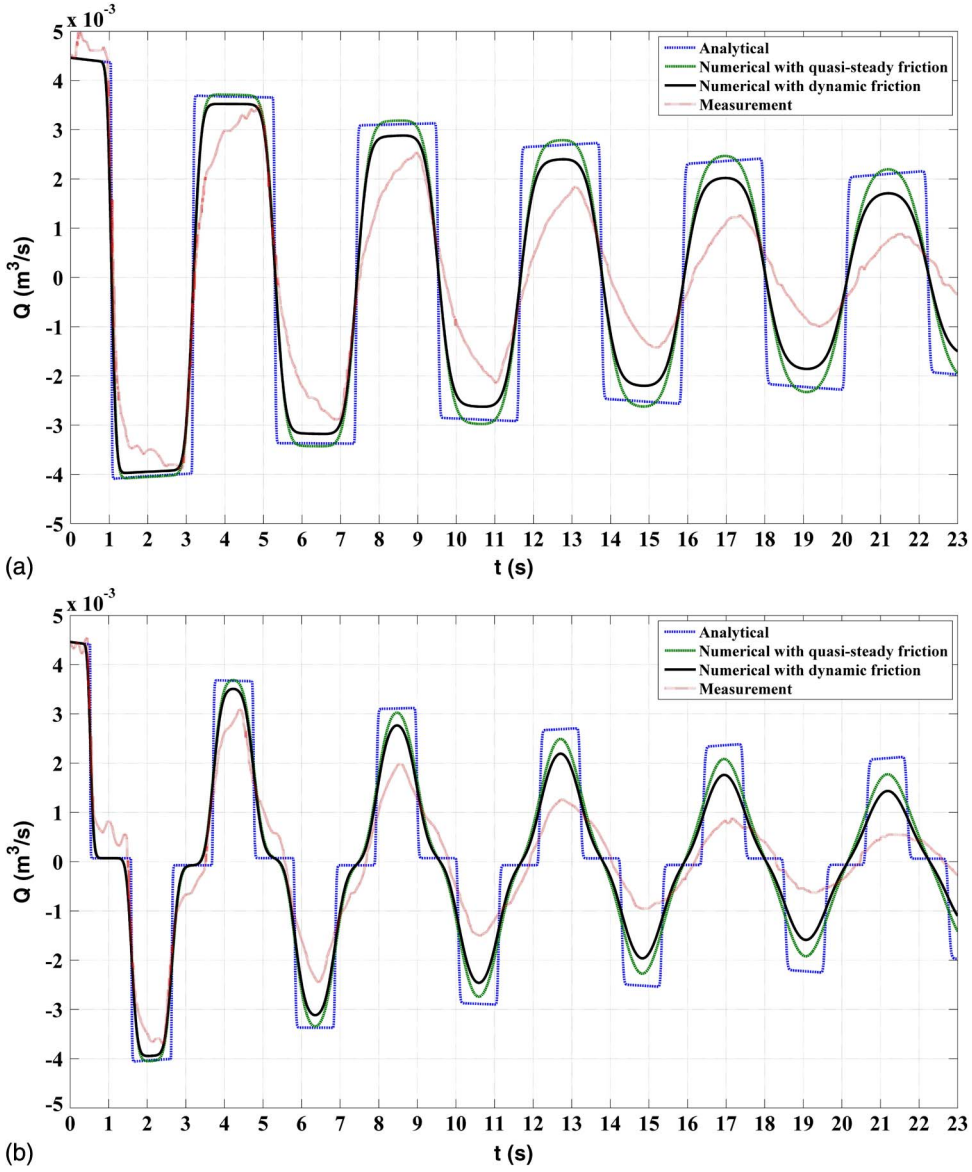

Fig. 7. Test no. 2: comparison of discharge profiles ($\Delta t = 0.002$ s, $N = 100$) between the various formulations for the friction term: (a) Section no. 1; (b) Section no. 2

steady friction only and of dynamic friction on wave attenuation in time. The findings indicate that inclusion of the dynamic friction reduces the peak water-hammer pressures when compared with the standard quasi-steady assumption for the friction. The inclusion of the dynamic friction results in a better agreement between calculated and measured values. In these two case studies, grid size and time step were reduced to test for convergence; the numerical solution presented is the converged solution. Computational time for each of the cases studied took only 3 min on a PC (operating system: Windows 7, 64 bits; CPU: Intel(R) Xeon(R) CPU E5620 @ 2.40 GHz x 2 processors; mainboard: ASUS Z8NA-D6(C); memory: 12280 MB triple channel DDR3 ECC @ 1333 MHz). Thus several variants may be studied in a short period of time. The efficient algorithm introduced in this paper may be adapted, with some modifications, to incorporate higher-order schemes that may yield less computational effort. Because the principal objective of this paper was to refine the physics of the phenomenon, extensive numerical experimentation with different schemes was not undertaken. However, for more precision in engineering applications, other key parameters such as cavitation, fluid–structure interaction, viscoelastic behavior of the pipe wall, leakage, and blockage have to be properly modeled and incorporated into the formulation. This paper may be used as a basis for the study of real mass variations in a surge tank. It should also prove useful as a tool for the optimal design of surge controls.

Acknowledgments

The authors gratefully acknowledge the partial financial support of Natural Sciences and Engineering Research Council of Canada (NSERC).

Notation

The following symbols are used in this paper:

$\mathbf{A}$ = Jacobian matrix of the flux $\mathbf{F}$ respecting to $\mathbf{U}$;

A_0 = cross-sectional area of pipe;

a = celerity of the pressure waves;

C^* = Vardy's shear decay constant;
D = diameter of the pipe;
d = (operator) differential;
E = Young's modulus of elasticity for the pipe material;
E_V = bulk modulus of elasticity;
e = pipe wall thickness;
$\mathbf{F}$ = vector flux in the x-direction;
f = friction factor;
f_q = quasi-steady part of the friction factor;
f_u = unsteady part of the friction factor;
k_S = absolute roughness of the pipe;
N = number of cells in the computational domain;
p = pressure;
Q = volume discharge;
Q_m = mass discharge;
$\mathbf{R}$ = matrix for the hyperbolic source term;
R = Reynolds number;
$\mathbf{S}$ = vector source term;
t = time;
$\mathbf{U}$ = vector variable;
V = fluid velocity;
x = unit vector in the x-direction;
Δt = computational time step;
Δx = cell size in the x-direction;
μ = mass of fluid per unit length of pipe; and
ρ = mass density.

Subscripts

b = value to be prescribed at a boundary;
b, L = value to be prescribed at the left-hand boundary;
b, R = value to be prescribed at the right-hand boundary; and
i = cell number.

Superscripts

n = time level;
n, h = numerical solution obtained at the time level n after the solution of the hyperbolic source term of the equation;
n, x = numerical solution obtained at the time level n after the solution of the conservation part of the equation in the x-direction;
$n + 1/2$ = Average value between the time level n and $n + 1$;
∞ = time level if t gets larger; and
$*$ = intermediate region in the solution of the Riemann problem.

References

Allievi, L. (1903). "Teoria generale del moto perturbato dell'acqua nei tubi in pressione (colpo d'ariete) [General theory of the variable motion of water in pressure conduits.]." *Annali della Società degli Ingegneri ed Architetti Italiani*, 17(5), 285–325 (in Italian).

Allievi, L. (1913). *Teoria del colpo d'ariete*, Tipografia della R. Accademia dei Lincei, Rome.

Allievi, L. (1932). *Il colpo d'ariete e la regolazione delle turbine*, Industrie grafiche italiane Stucchi, Milano, Italy.

Anderson, A. (1976). "Menabrea's note on waterhammer: 1858." *J. Hydraul. Div.*, 102(1), 29–39.

Bergant, A., Ross Simpson, A., and Vìtkovsk, J. (2001). "Developments in unsteady pipe flow friction modelling." *J. Hydraul. Res.*, 39(3), 249–257.

Bergant, A., Tijsseling, A. S., Vítkovský, J. P., Covas, D. I., Simpson, A. R., and Lambert, M. F. (2008a). "Parameters affecting water-hammer wave attenuation, shape and timing. I: Mathematical tools." *J. Hydraul. Res.*, 46(3), 373–381.

Bergant, A., Tijsseling, A. S., Vítkovský, J. P., Covas, D. I., Simpson, A. R., and Lambert, M. F. (2008b). "Parameters affecting water-hammer wave attenuation, shape and timing. II: Case studies." *J. Hydraul. Res.*, 46(3), 382–391.

Bousso, S., and Fuamba, M. (2013). "Numerical simulation of unsteady friction in transient two-phase flow with Godunov method." *J. Water Resour. Prot.*, 5(11), 1048–1058.

Brunone, B., and Berni, A. (2010). "Wall shear stress in transient turbulent pipe flow by local velocity measurement." *J. Hydraul. Eng.*, 10.1061/(ASCE)HY.1943-7900.0000234, 716–726.

Brunone, B., Golia, U., and Greco, M. (1991). "Modelling of fast transients by numerical methods." *Proc., Int. Conf. on Hydraulics Transients with Water Column Separation*, IAHR, Valencia, Spain, 273–280.

Chaudhry, M. (1987). *Applied hydraulic transients*, Van Nostrana Reinhold Co., New York.

Chaudhry, M. H., Sabbah, M. A., and Fowler, J. E. (1985). "Analysis and stability of closed surge tanks." *J. Hydraul. Eng.*, 10.1061/(ASCE)0733-9429(1985)111:7(1079), 1079–1096.

Chaudhry, M. H., and Silvaaraya, W. F. (1992). "Stability diagrams for closed surge tanks." *Proc., Int. Conf. on Unsteady Flow and Fluid Transients*, HR Wallingford Ltd. and IAHR, Durham, U.K., 221–228.

Finnemore, E., and Franzini, J. (2002). *Fluid mechanics with engineering*, 10th Ed., McGraw-Hill, New York.

Gallerano, F., and Cannata, G. (2011). "Central WENO scheme for the integral form of contravariant shallow-water equations." *Int. J. Numer. Methods Fluids*, 67(8), 939–959.

Gallerano, F., Cannata, G., and Tamburrino, M. (2012). "Upwind WENO scheme for shallow water equations in contravariant formulation." *Comput. Fluids*, 62, 1–12.

Guinot, V. (2003). *Godunov-type schemes: An introduction for engineers*, Elsevier, Amsterdam.

Harten, A., Engquist, B., Osher, S., and Chakravarthy, S. R. (1987). "Uniformly high order accurate essentially non-oscillatory schemes, III." *Upwind and high-resolution schemes*, Springer, New York, 218–290.

Jaeger, C. (1933). "Théorie générale du coup de bélier." Diss. Techn. Wiss. ETH Zürich, Zürich, Switzerland.

Jiang, G. S., and Shu, C. W. (1995). "Efficient implementation of weighted ENO schemes." *Technical Rep. ICASE 995-73*, ICASE, Hampton, VA.

Kim, S. H. (2010). "Design of surge tank for water supply systems using the impulse response method with the GA algorithm." *J. Mech. Sci. Technol.*, 24(2), 629–636.

Lescovich, J. E. (1967). "The control of water hammer by automatic valves." *J. Am. Water Works Assoc.*, 59(5), 632–644.

Liu, X. D., Osher, S., and Chan, T. (1994). "Weighted essentially non-oscillatory schemes." *J. Comput. Phys.*, 115(1), 200–212.

Menabrea, L. F. (1858). *Note sur les effets du choc de l'eau dans les conduites*, Mallet-Bachelier, Paris.

Michaud, J. (1878). "'Coups de bélier dans les conduites, Étude des moyens employés pour en atteneur les effects." *Bull. Soc. Vaudoise Ing. Arch.*, 4(3), 4.

Michaud, J. (1903). *Intensité des coups de bélier dans les conduites d'eau*, H. Vallotton & Toso, Lausanne, Switzerland.

Moghaddam, M. A. (2004). "Analysis and design of a simple surge tank (research note)." *Int. J. Eng. Trans. A: Basics*, 17, 339–345.

Osher, S., and Chakravarthy, S. (1984). "High resolution schemes and the entropy condition." *SIAM J. Numer. Anal.*, 21(5), 955–984.

Park, J. S., Yoon, S. H., and Kim, C. (2010). "Multi-dimensional limiting process for hyperbolic conservation laws on unstructured grids." *J. Comput. Phys.*, 229(3), 788–812.

Ramadan, A., and Mustafa, H. (2013). "Surge tank design considerations for controlling water hammer effects at hydro-electric power plants." *Univ. Bull.*, 15(3), 147–160.

Roche, E. (1975). "Assainissement rural: Protection des conduites de refoulement." *TSM l'Eau*, 365–378.

Schnyder, O. (1932). "Uber druckstosse in rohrleitungen." *Wasserkraft und Wasserwirtschaft*, Springer, Berlin.
Seck, A., and Fuamba, M. (2015). "Contribution to the analytical equation resolution using charts for analysis and design of cylindrical and conical open surge tanks." *J. Water Resour. Prot.*, 7(15), 1242–1256.
Shamloo, H., and Mousavifard, M. (2015). "Numerical simulation of turbulent pipe flow for water hammer." *J. Fluids Eng.*, 137(11), 111203.
Shamloo, H., Norooz, R., and Mousavifard, M. (2015). "A review of one-dimensional unsteady friction models for transient pipe flow." *Cumhuriyet Sci. J.*, 36(3), 2278–2288.
Shu, C. W. (1998). *Essentially non-oscillatory and weighted essentially non-oscillatory schemes for hyperbolic conservation laws*, Springer, New York.
Streeter, V. L., and Wylie, E. B. (1993). *Fluid transients in systems*, Prentice-Hall, Englewood Cliffs, NJ.
Titarev, V., and Toro, E. F. (2003). "On the use of TVD fluxes in ENO and WENO schemes." *Technical Rep. UTM 635*, Matematica, Univ. of Trento, Trento, Italy.
Toro, E. F. (2001). *Shock-capturing methods for free-surface shallow flows*, Wiley, New York.
Trikha, A. K. (1975). "An efficient method for simulating frequency-dependent friction in transient liquid flow." *J. Fluids Eng.*, 97(1), 97–105.
Vardy, A., and Brown, J. (2003). "Transient turbulent friction in smooth pipe flows." *J. Sound Vib.*, 259(5), 1011–1036.
Zielke, W. (1968). "Frequency-dependent friction in transient pipe flow." *J. Basic Eng.*, 90(1), 109–115.
Zijlema, M., and Wesseling, P. (1998). "Higher-order flux-limiting schemes for the finite volume computation of incompressible flow." *Int. J. Comput. Fluid Dyn.*, 9(2), 89–109.